

Improvement of optical damage in specialty fiber at 266 nm wavelength

T. Tobisch⁴, H. Ohlmeyer^{1,4}, H. Zimmermann², S.Prein², J. Kirchhof³, S.Unger³,
M. Belz⁴, K.-F.Klein^{1,4}

¹ Technische Hochschule Mittelhessen - University of Applied Sciences,
W.-Leuschner-Str. 13, 61169 Friedberg, Germany

email: Karl-Friedrich.Klein@iem.thm.de

² CryLaS GmbH, Ostendstr, 25, 12459 Berlin, Germany

³ IPHT Jena, Albert-Einstein-Str.9, 07745 Jena, Germany

⁴ TransMIT GmbH, Center of fiber-optics and industrial laser applications,
Saarstr. 23, 61169 Friedberg, Germany

ABSTRACT

Improved multimode UV-fibers with core diameters ranging from 70 to 600 μm diameter have been manufactured based on novel preform modifications and fiber processing techniques. Only E'-centers at 214 nm and NBOHC at 260 nm are generated in these fibers.

A new generation of inexpensive laser-systems have entered the market and generated a multitude of new and attractive applications in the bio-life science, chemical and material processing field. However, for example pulsed 355 nm Nd:YAG lasers generate significant UV-damages in commercially available fibers. For lower wavelengths, no results on suitable multi-mode or low-mode fibers with high UV resistance at 266 nm wavelength (pulsed 4th harmonic Nd:YAG laser) have been published. In this report, double-clad fibers with 70 μm or 100 μm core diameter and a large cladding-to-core ratio will be recommended. Laser-induced UV-damages will be compared between these new fiber type and traditional UV fibers with similar core sizes. Finally, experimental results will be cross compared against broadband cw deuterium lamp damage standards.

Keywords: step-index fibers, multimode fibers, fiber-optic delivery system, UV-defects, UV-applications, 266 nm laser

1. INTRODUCTION

Defects in silica [1-4] can be generated by ionizing radiation like Gamma-rays, X-rays or DUV-light. Spectral UV-induced losses in the UV-region have been determined with deuterium-lamp or excimer-lasers, for the last two decades. Only some optically active defects were commonly observed in undoped synthetic silica (Table 1) in [5,6,7]. Especially the E'-center with an absorption band at 215 nm and the Non-Bridging-Oxygen-Hole center (NBOHC) at 260 nm in high-OH silica are well described in the literature. Many studies on silica-based fibers have been carried out to show the influence of preform manufacturing, especially silica deposition of the core and cladding material, and the drawing process. In addition, Oxygen-Deficient-Centers (ODCs) generating absorbing bands around 250 nm were observed in low-OH silica. Thorough reviews on UV-defects including references can be found in the recent literature [2-5, 8-10].

The spectral stability of multimode step-index UV-fibers have been improved over decades. This research focused on step-index fiber with undoped core and F-doped cladding and core diameters between 200 μm and 600 μm , using characterization based on deuterium lamps exhibiting a broadband spectrum in the DUV region [11-13]. Further, several studies had been carried out with pulsed excimer lasers, e.g. [14-16]. In parallel, characterization techniques were developed and refined. Currently, this work in parallel is used as a basis for a standardization of UV-damages reporting of silica-based fibers [6,11,12,17].

With the introduction of new low-cost pulsed Nd:YAG lasers (355 & 266 nm), a range of new UV applications in the material processing, chemical and bio-life science field become possible. As a result of improved beam quality, fibers with smaller core diameters and higher UV stability are required. In addition to improved standard 100 μm core fibers, double-clad fibers with 70 μm or 100 μm core diameter and a large cladding-to-core ratio have been developed. These were tested with pulsed 355 nm Nd:YAG lasers (third harmonics) and a high-power cw broadband plasma lamp [7]. A different degradation mechanism was found and is shown in Fig.1. In respect to deuterium-lamps, two statements for 355 nm lasers are obvious: a) the laser-induced UV losses are higher; b) the 260 nm band is significantly higher, especially for high pulsed lasers with 20 μJ /pulse @ 100 Hz (table 1 in [18]). However, the UV-damage was significantly reduced using hydrogen in the light-guiding area [7]. Further, it was found that these mechanisms are strongly temperature-dependent (see Fig. 2, [19]).

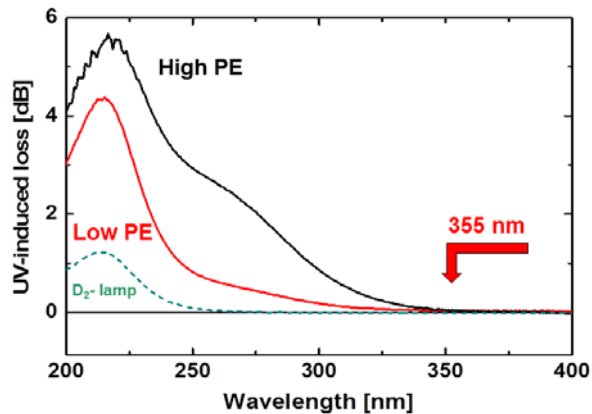


Fig. 1: Spectral UV-damage of 2 m long UV-improved FDP-fibers with 100 μm core, after 4 h UV irradiation, using different 355 nm pulsed Nd:YAG lasers with different pulse energies and fluences, in comparison to deuterium lamp (lower curve, dashed); pulse energy: 20 μJ or 250 mJ/cm^2 (high PE, upper curve), 1.5 μJ or 20 mJ/cm^2 (low PE, curve in the middle); more details in [7,19]

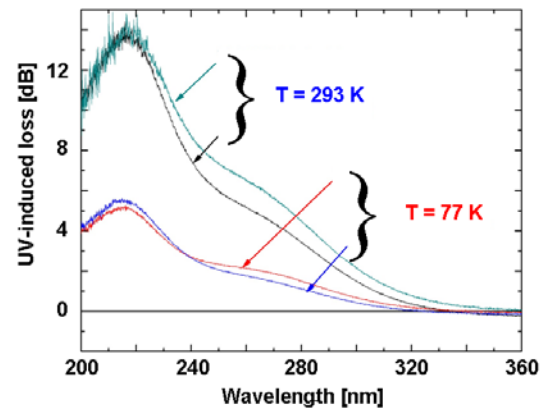


Fig. 2: Temperature-dependent loss of 5 m long UV-improved FDP-fibers with 100 μm core, after 4 h UV irradiation, using different 355 nm pulsed Nd:YAG lasers with high power pulse energies (see Fig. 1); tests were carried out at room temperature (293 K) and at liquid-nitrogen (77 K); more details in [7,19]

In addition to 355 nm wavelength, the pulsed Nd:YAG lasers with 266 nm (fourth harmonics), are used in the following applications: MALDI-TOF, micro dissection, laser induced fluorescence (LIF), light detection and ranging (LIDAR), micro machining, marking, and basic research in bio-photonics and life science. They are also used as replacement for Nitrogen gas lasers when high reliability and low service cost is a requirement. With smaller spot-sizes, however, non-linear absorption has to be taken into account. In this paper, the reduction of UV-damage of these fibers with smaller diameter ($\leq 100 \mu\text{m}$ core diameter) will be described in more detail at this wavelength.

2. PULSED ND:YAG LASER WITH 266 NM WAVELENGTH

Based on a diode pumped passively Q-switched Nd:YAG laser with internal frequency conversion stage, the FTSS355-Q and FQSS266-Q series lasers of CryLaS offer reliable radiation at 355 nm (see table 1 in [18]) and 266 nm (see table 1), respectively. Due to the microchip design the lasers are very compact, robust and simple to integrate. Various models are available with different pulse energies up to 40 μJ or different repetition rates up to 20 kHz. The repetition rate can be varied either by the included software or through an external trigger signal. Due to the short pulse width of approx. 1 ns the peak power reaches values up to 11 kW while the maximum average power is up to 11 mW. All lasers are equipped with an internet based remote service interface which allows adjustment of critical parameters of units in the field. The lasers are available as stand-alone systems and as OEM units for simple integration in complex systems.

In Fig. 3, photographs of different 266 nm laser used in the following experiments are shown. A fiber-coupler can be integrated, too.

In the first tests, the repetition rate was 1 kHz. The average output power of the lasers used was as follows: 0.7 mW (Q2) and 11 mW (Q3).



Fig. 3: Photographs of different 266 nm lasers [20]: FQSS266-Q2 (A), new FQSS266-Q3 (B), laser head with fiber-coupler (C)

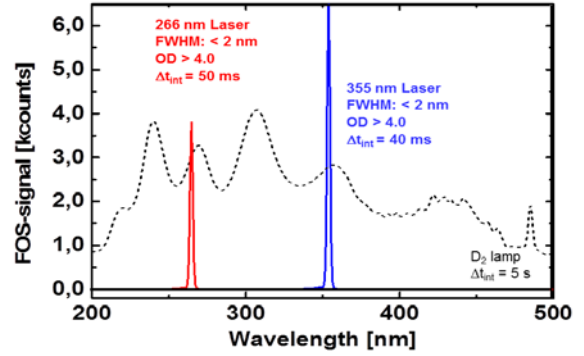


Fig. 4: Spectral output power with for different light sources used in these studies, measured with the same fiber-optic spectrometer [21], but different integration times and additional attenuators: deuterium lamp (dashed line, $\Delta t_{int} = 5$ s), the high pulse-power 266 and 355 nm laser ($\Delta t_{int} = <50$ ms, Neutral filter with $OD > 4.0$)

The spectra of the lasers were measured in comparison to the standard deuterium lamp. The signal of the fiber-optic spectrometer (FOS) is proportional to the output power; however, the proportional factor is wavelength-dependent (see section 3.2). Because of different levels of spectral power, the integration time Δt_{int} for the photo-diode array used in the spectrometer was adjusted. While this time was 5.0 s (maximum) for deuterium lamp, it was reduced by a factor of >100 for the pulsed Nd:YAG laser at 266 wavelength under test; however, the laser beam had to be additionally attenuated by neutral density filters ($OD > 4.0$). Taking the spectra in Fig. 4 in account, the averaged spectral power [unit: $\mu\text{W}/\text{nm}$] is more than 40 dB higher at both wavelengths in respect to the deuterium lamp.

Table 1: Summary of 266 nm lasers used [20]

Model	FQSS266-Q2	FQSS266-Q3 (new)
Pulse energy (max)	$> 1.25 \mu\text{J} @ 1 \text{ kHz}$	$> 6.0 \mu\text{J} @ 1 \text{ kHz}$
Pulse duration	$\leq 1.0 \text{ ns}$	$\leq 1.0 \text{ ns}$
Beam divergence	$< 2.0 \text{ mrad}$	$< 2.0 \text{ mrad}$
Beam dimension	$0.85 \text{ mm} \pm 0.15 \text{ mm}$ (output coupling window)	$0.80 \text{ mm} \pm 0.2 \text{ mm}$ (output coupling window)
Max. repetition rate	2.5 kHz	2.5 kHz
Pulse peak power	$> 1.25 \text{ kW} @ 1 \text{ kHz}$	$> 6 \text{ kW} @ 1 \text{ kHz}$
Average laser power (at max. rep. rate)	$> 1.25 \text{ mW} @ 1 \text{ kHz}$	$> 6 \text{ mW} @ 1 \text{ kHz}$

3. USED FIBERS AND TEST-EQUIPMENTS

3.1 Specialty UV-fibers under test

Because of the higher power and power densities of new light-sources, step-index multimode UV-fibers with smaller core diameters can be used in light delivery-systems. In first step, UV fibers with 70 and 100 μm core diameter and core-cladding-ratio (CCR) have been characterized (fiber #1-4), from different generations [6,7]. These fibers have been manufactured in the following way [23]: silica core with high-OH content made by flame hydrolysis, fluorine doped cladding made by plasma outside deposition and Polyimide-coating cured during fiber drawing.

For longer UV stability, UV-fibers were produced with significantly higher CCR (= 5.0). The special fibers (fiber #5-8) are based on the improved SBU-preform (CCR 1.1 [23]) which was overladded by an un-doped silica F300 tube [23] to reach the CCR of 5.0. This R&D preform has been manufactured at IPHT [24]. From this preform, two fibers with 70 μm and 100 μm core diameters were drawn. In addition, hydrogen loading can be applied (see table 2). Details about hydrogen fibers and their behavior are given in SPIE2013, [12,13,25,26]. In the following, the fiber lengths are mainly the same: 2.0 m.

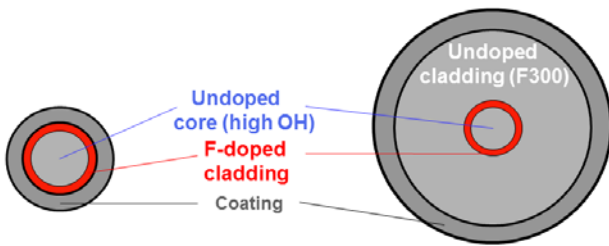


Fig. 5: Cross-section area of standard UV-fibers (# 1-4) with CCR <1.2 (typical value: 1.1) and R&D UV-fibers (# 5-8) with large CCR = 5.0; for longer lifetime, fiber 6 & 8 were hydrogen-loaded; the numerical aperture (typical perform values: 0.22 @ 633 nm [23]) are the same at operation wavelength of 266 nm, for all fibers

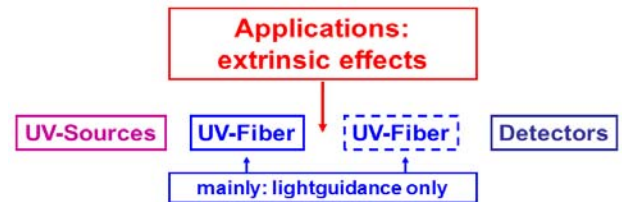


Fig. 6: Overview of a fiber-optic system for UV-applications, which can be used for measuring the UV-damage of multi-mode silica-based fibers (see table 2)

Table 2: Tested UV-fibers with different cladding-core-ratios, core material and hydrogen-content [23,24,27,28]; *: trade names [27]

Fiber #	Type	Core diameter	CCR1	CCR2	Length	Comments
1	FVP*	100 μm	1.1	-	1 m	1 st generation
2	UVM*	200 μm	1.1	-	2 m	3 rd generation
3	FDP*	<100 μm	1.1	-	2 m	4 th generation
4	FDP*	100 μm	1.1	-	2 m	4 th generation
5	R&D	70 μm	1.1	5.0	2 m	without loading
6	R&D	70 μm	1.1	5.0	2 m	hydrogen-loaded
7	R&D	100 μm	1.1	5.0	2 m	without loading
8	R&D	100 μm	1.1	5.0	2 m	hydrogen-loaded

3.2 Existing equipments for UV-damage

For UV-damage, two systems were built up. In principle, the damaging systems contain the UV-source (deuterium-lamp or 266 nm laser), the fiber under test and the detection systems (Fig. 6); however, a second fiber was not used. Typically, the fiber lengths were chosen to be 2.0 m.

Both light-sources were focused onto the fiber front-face with an imaging system, consisting of UV lenses.

Using the cw broadband deuterium-lamp [22] as reference, the output power was detected with a silicon-detector including band-pass filters or with the fiber-optic spectrometer TIDAS [21]. With a shutter in between the fiber and the light-source, the drift of dark signal and the annealing of the fiber after UV-irradiation are monitored. Details see [6].

Using the two 266nm pulsed lasers, the averaged output power and the pulse energy were temporally monitored with thermopile or pyro-electric detectors. For spectral analyses of UV-damage, the treated fibers were tested in the system described above with deuterium-lamp; however, the irradiation time was less than 5 s to avoid further damage or annealing (see [7,19]).

The measured signal of the fiber-optic spectrometer (FOS) is proportional to the optical power; however, the proportional factor is influenced by the coupling-efficiency, the grating transmission and the sensitivity of the photo-diodes which are wavelength-dependent. Therefore, the FOS-signal (in counts per integration time) can be used for difference analyses, with high accuracy.

4. EXPERIMENTAL RESULTS

4.1 UV-damage with laser FQSS266-Q2

Although the different fibers in table 1 were studied, the following results will be focused on the 4th generation of UV-fibers (FDP-type with cladding-to-core-ratio (CCR) = 1.1), as shown already in Fig. 1 & 2 for 355 nm laser damage, and on the R&D-samples with same core diameters, but higher CCR (= 5.0). Using the laser FQSS266-Q2 (table 1) with approx. 0.70 mW input, the spectral and temporal behavior of the UV-induced losses at 214 and 266 nm are quite different (Fig. 7), compared to the same losses generated by the high damaging deuterium lamp (see Fig. 1), described in [6,7]. First of all, there is a significantly higher concentrations of E'- and NBOH centers. On the other hand, as seen in Fig. 1, the high pulse power laser at 355 nm had generated both defects, too; however, the absorption values are approx. 2.6 (@ 214 nm) and 3.4 (@ 266 nm) times smaller compared to the damage generated by the 266 nm laser after 4 h irradiation.

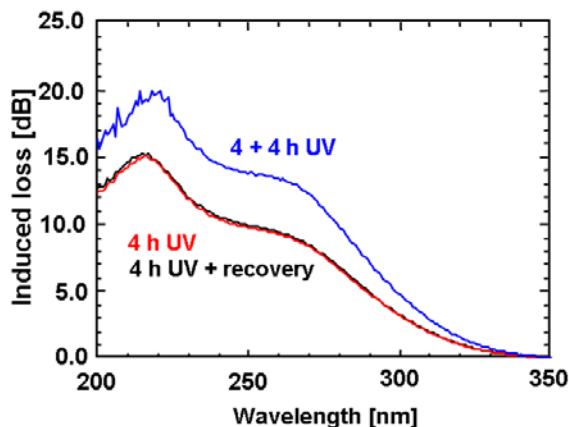


Fig. 7: Laser-induced damage of non-loaded FDP-fiber (fiber #3, 4th generation) for different damaging times (4 & 8 h) with 266 nm laser (laser output power: 0.7 mW), measured off-line with the measurement system for UV damage [6] including the fiber-optic spectrometer [21]; after first laser-irradiation, 16 hours recovery without any illumination showed nearly no spectral changes

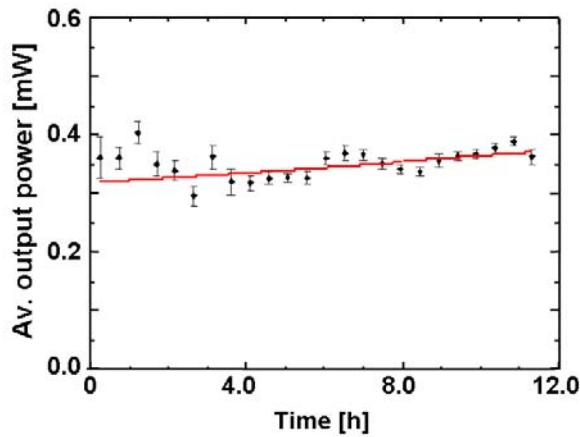


Fig. 8: Temporal output power of hydrogen-loaded R&D-fiber (fiber #6) for laser wavelength 266 nm (laser output power: 0.7 mW); taking the losses into account, the input power behind the fiber front face was 0,42 mW (estimated)

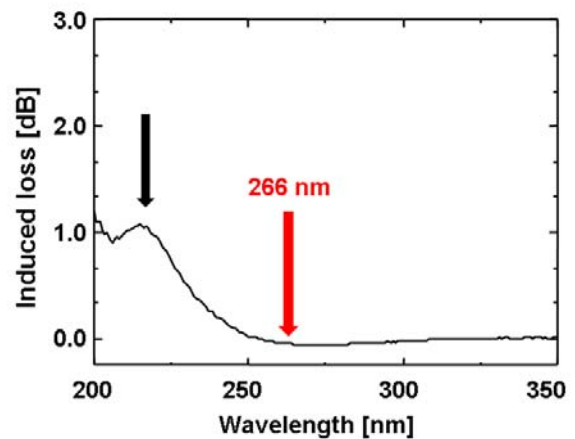


Fig. 9: Spectral laser-induced damage of hydrogen-loaded R&D-fiber (fiber #6) after 12 hours of irradiation with 266 nm laser (laser output power: 0.7 mW), measured off-line with the measurement system for UV damage [6]

No UV-damage at 266 nm was observed over a period of 12 hours using the loaded R&D-samples (Fig. 8). The averaged output power was 0.35 mW. With a basic attenuation at 266 nm of 0.25 dB/m (typical value in un-doped silica fibers), the averaged input power into the fiber was estimated: 0.42 mW. Taking the Fresnel losses at the fiber front face and lens-system into account, the coupling efficiency of the laser beam can be determined: the value of 70% into a 70 μm core is acceptable.

After 12 h laser irradiation, the spectral UV-damage of the 2 m long sample was measured (Fig. 9). As expected, no laser-induced loss was observed at 266 nm; even, a small gain at 266 nm (< 0.1 dB) can be determined. However, the 214 nm loss with approx. 1.1 dB is relatively strong; so far, this absorption band should be passivated in the presence of hydrogen [11-13]. Further temporal studies at different temperatures will help to understand this phenomenon.

4.2 UV-damage with laser FQSS266-Q3

With the new FQSS266-Q3, damage tests with higher pulse energies and averaged power levels were carried out (Fig.10 & 11). In this case, the hydrogen-loaded fiber #8 with 100 μm core diameter in the assemblies TZ 03070 was under test. As indicated by the farfield pattern at fiber output, the radial position of the focus point on the front-face was quite different: nearly in the center ($r = 0$ μm) vs. close to the core-cladding interface (estimated: $r > 30$ μm). However, the output power was nearly the same in steady-state: approx. 3.0 $\mu\text{J}/\text{pulse}$ at a repetition rate of 1 kHz. After a drop of approx. 25% within the first 1 hour (not shown), the output power is nearly stable. In Fig 10, there is a tendency of further marginal reduction of output pulse energies noticeable. As indicated by the far-field pattern at fiber output, the radial position of the laser focus was not in the fiber center (see [29]). After new adjustment of the focus in radial direction, leading to a more homogeneous far-field pattern, a higher stability was observed (Fig. 11).

For these tests, the pulse energy of the laser was fixed: 11 μJ . Due to losses in the imaging system, the pulse energy at fiber front-face was 9.2 μJ . Taking Fresnel losses into account, total transmission was approx. 35%.

For decreasing wavelength, non-linear effects are no longer negligible, as described in detail in [13-16]. In our tests, the output power was nearly the same for input pulses with energies greater than 5.0 $\mu\text{J}/\text{pulse}$ coupled into a 100 μm core fiber. On the other hand, first results of surface damage on fiber input were received (Fig. 12), which may be the dominant factor for the maximum output power using an attenuator in front of the fiber and a spot size of approx. 40 μm , mechanical damages were observed after approx. 140 min equivalent to 8.4 million pulses, even at 3 $\mu\text{J}/\text{pulse}$ or 3 kW peak power. As seen in Fig. 12, too, changing the focus position on the front face at approx. 200 min a non-damaged area could be found with the same coupling efficiency (approx. 60%) in comparison to the beginning of the test.

With the spot-size of approx. 40 μm , estimated by the lens-systems, the following data are derived: 240 W/cm² average power density, 0.24 J/cm² pulse energy density and 240 MW/cm² peak power density.

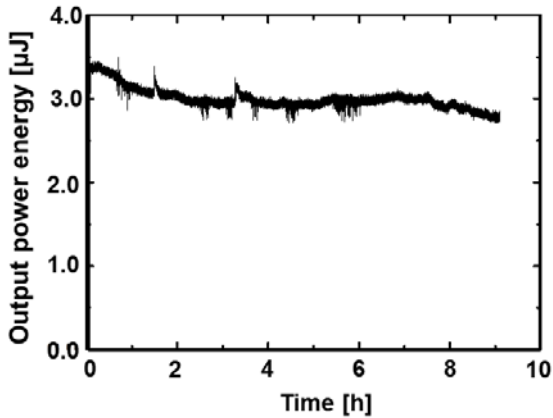


Fig. 10: Temporal output pulse energies of the assembly TZ03070 with hydrogen-loaded R&D-fiber (fiber #8) for laser wavelength 266 nm (laser output pulse energy: 11 μJ); input condition: laser focus close to core-cladding interface

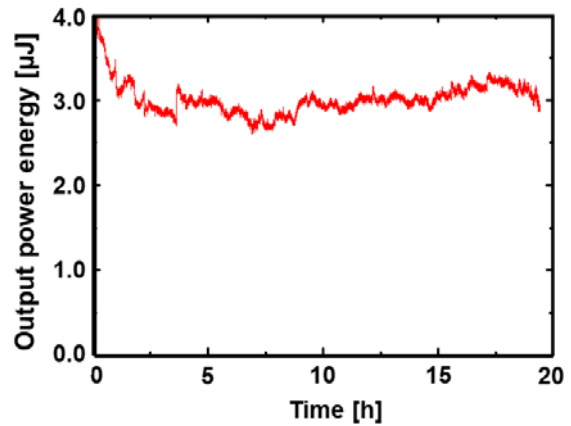


Fig. 11: Temporal output pulse energies of the assembly TZ03070 with hydrogen-loaded R&D-fiber (fiber #8) for laser wavelength 266 nm (laser output pulse energy: 11 μJ); input condition: laser focus in the center of the fiber

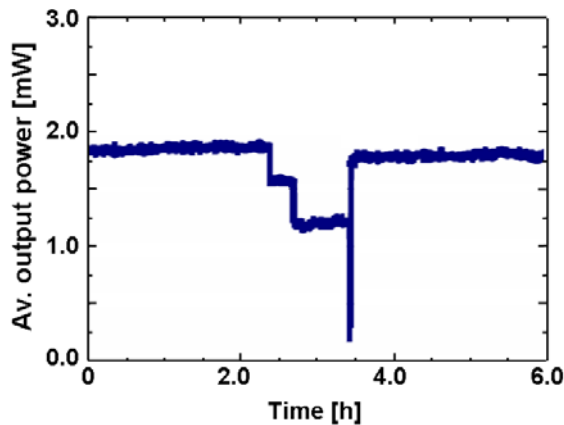


Fig. 12: Temporal output pulse energies of the assembly TZ03071 with hydrogen-loaded R&D-fiber (fiber #8) for laser wavelength 266 nm (fiber input pulse energy: 3.0 μJ); input condition: variable due to re-alignment

4.3 Long-term UV-damage with deuterium-lamp

Using 266 and 355 nm pulsed lasers, the appearance of the NBOHC with an absorption maximum at 260 nm (and 630 nm) wavelength was significant. In addition, the loss at 260 / 266 nm was not saturated within the standard test duration of 4 hours, if the deep UV-power of a deuterium-lamp was increased by nitrogen-purge between lamp and fiber input.

Stimulated by these results, further studies with the broadband D2-lamps were carried out. As shown in Fig. 13, a pretended 266 nm plateau, after 15 minutes of UV irradiation, is not real for the FDP-fibers with 100 μm core diameter or smaller (fiber #3 & 4). Measuring the UV-damage for 48 hours, the loss is increasing with a rate of approx. 0.02 dB/h, after the first significant step of approx. 0.2 dB in a 2 m long fiber. The 214 nm absorption band is not stable, too. After a local maximum of approx. 1.0 dB at approx. 20 min and a minimum at approx. 7 hours, the induced losses at 214 nm are increasing again, with a rate in the order of 0.01 dB/h.

The spectral shape is changing over time, significantly. As shown in Fig. 14, the 266 nm loss will have the same value as the 214 nm loss, after 48 hours. So far, longer tests have not been carried out. Therefore, no statement about the stability of the spectral fiber transmission seems to be possible at this moment.

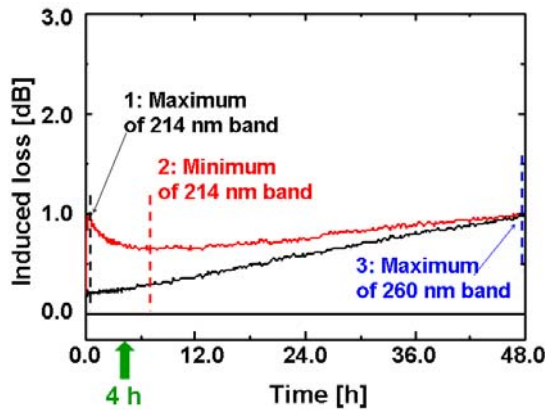


Fig. 13: Temporal UV-damage of the improved UV-fiber (FDP-type; fiber #3 & 4 without hydrogen loading); fiber data: 100 or <100 μm core diameter, CCR = 1.1 and 2.0 m length

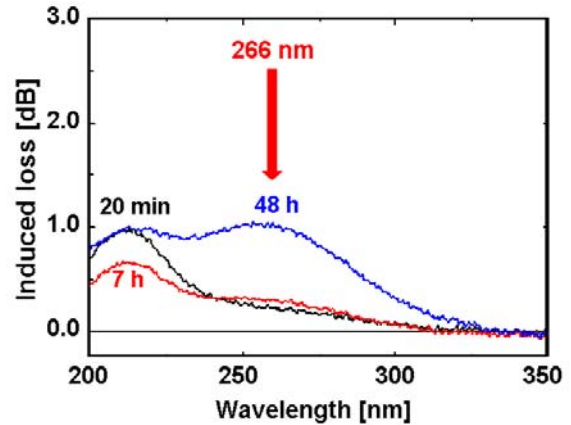


Fig. 14: Spectral UV-damage of the improved UV-fiber (FDP-type; fiber #3 & 4 without hydrogen loading), after 20 min, 7 & 48 hours; the same raw data as in Fig. 13 are used

4.4 Discussion

The standard FDP-fiber (4th generation) with 100 μm core and the non-loaded R&D-fiber with 70 μm core, especially developed for UV laser applications, show similar behavior in respect to temporal and spectral UV-induced losses.

With the broadband deuterium-lamp, the E'-centers are mainly generated in the core region by absorption of single photons with energies $> 5.8 \text{ eV}$ ($< 214 \text{ nm}$ wavelength). The UV-light above 225 nm is not relevant for the damaging process at 214 nm, as shown in [6,7]. However, it has to be taken into account in all measurements with deuterium-lamp that the defect concentration depends on the position in the fiber (z-direction) due to the spectral changes of the damaging spectra along the fiber [6].

Due to two-photon absorption, the 266 nm laser light can degrade the fiber in the wavelength region below 250 nm. In addition to Non-Bridging-Oxygen-Hole centers (NBOHC) with an absorption maximum close to the laser wavelength, the E'-centers at 214 nm are generated, too. The concentrations of both defects are increasing with increased pulse energies or averaged power densities.

As expected, the hydrogen-loaded fibers have significantly improved UV resistance. The UV-induced losses at 266 nm will be extremely low for quite a while (expectation for 100 μm core diameter at room temperature: > 9 months), because out-gassing of hydrogen out of the core region is significantly reduced [30] due to the large cladding-to-core ratio (CCR). The losses in a 2 m long fiber were mainly below 0.1 dB at this wavelength. However an absorption band around 214 nm was not passivated totally, although molecular hydrogen was available in high concentrations.

5. SUMMARY AND OUTLOOK

In this paper, UV-damage in silica based UV-fibers has been studied in detail. The core diameters of these fibers under test were only 70 and 100 μm . However, the cladding-to-core ratio was chosen quite differently to include long-term hydrogen-passivation: especially the CCR of 5.0 is a good compromise between fiber flexibility and life time, after hydrogen-loading.

Using low-power deuterium lamp and pulsed 266 nm Nd:YAG lasers, the UV-induced losses of the specialty R&D fibers without any additional hydrogen-loading was similar to the values achieved with 200 and 600 μm core fibers. However, in addition to the E'-centers (214 nm) the Non-Bridging Oxygen Hole center (NBOHC, 260 nm in the UV-region) will be generated. Due to the deep UV spectrum of the D₂-lamp, single photon absorption is possible for fiber damaging. On the other hand, two photon absorption of pulsed laser light is beneficial to generate UV-defects. The concentration of these defects is strongly dependent on the power or pulse energy in specific wavelength regions; therefore, a length-dependency has to be taken into account, too.

Future work will concentrate on the non-linearities, including two-photon absorption and Raman-scattering, and surface damage in the R&D fiber; in this paper, only preliminary results for these fluence-dependent effects on the fiber transmission were shown. In further studies, the new experimental results will be compared with values predicted by 266 nm data given in [15,16].

For high and stable fiber transmissions, the power density in the fiber has to be reduced. Therefore, laser systems with higher repetition rates and lower pulse energies are favorable for new applications, as long as the average power is important.

6. ACKNOWLEDGEMENT

We would like to thank J. Clarkin, V. Khalilov, J. Shannon, and R. Timmerman (Polymicro Technologies, Phoenix) for fruitful discussions about improvement of UV-fibers and measurement techniques, C. Jakob and S. Backfisch (TransMIT, Friedberg) for testing some of the samples. Finally, we acknowledge the sustained support by G. Hillrichs (Hochschule Merseburg).

7. REFERENCES

- [1] D.L.Griscom: „Defect structures of glasses“. J.Non-Cryst. Solids. Vol. 73, pp. 51-78 (1985)
- [2] E.J.Friebele, D.L.Griscom: "Radiation effects in glass" in "Treatise on material science and technology". Acad.Press, New York, pp. 257-351 (1979)
- [3] E.J.Friebele, et.al.: "Overview about Radiation Effects in Fiber Optics". SPIE-proc. 541, pp. 70 (1985)
- [4] R.A.Weeks: "The many varieties of E'-centers: a review". J.-Non-Cryst.Solids, Vol. 179, pp. 1-9 (1994)
- [5] V.Khalilov, J.Shannon, R.Timmerman: "Improved Deep UV Fiber for Medical and Spectroscopy Applications". SPIE-Proc. BiOS'14, Vol. 8938, paper 8938-9 (San Francisco, USA, Jan. 2014)
- [6] K.-F.Klein, C.P.Gonschior, D.Beer, H.-S.Eckhardt, M. Belz, J.Shannon, V.Khalilov, M.Klein, C.Jakob: "Silica-based UV-fibers for DUV applications: current status". SPIE-Proc., Vol. 8775, paper 8775-10 (Prague, Czechia, April 2013)
- [7] J.Heimann, K.-F.Klein, C.P.Gonschior, Moritz Klein, G.Hillrichs: "Optical fibers for 355 nm pulsed lasers and high-power broadband light sources". SPIE-Proc. BiOS'13, Vol. 8576, paper 8576-19 (San Francisco, USA, Jan. 2013)
- [8] Skuja: "Optically active oxygen-deficiency-related centers in amorphous silicon dioxide". J.-Non-Cryst.Solids, Vol. 239, pp. 16-48 (1998)
- [9] V.Kh.Khalilov, G.A.Dorfman, E.B.Danilov, M.I.Guskov, V.E.Ermakov: "Character, mechanism of formation and transformation point defects in type IV silica glass". J.-Non-Cryst.Solids, Vol. 169, pp. 15-28 (1994)
- [10] M.Belz, H.-S.Eckhardt, C.P. Gonschior, G.Nelson, K.-F.Klein: "Quality control of UV resistant fibers for 200-300 nm spectroscopic applications".SPIE-Proc.Vol. 6852 (BiOS 08), paper 6852-33 (San Jose, Jan. 2008)
- [11] K.F.Klein,P.Schliessmann,E.Smolka,M.Belz,W.J.O.Boyle,K.T.V.Grattan: "UV-stabilized silica based fiber for application around 200 nm wavelength". Sensors and Actuators B, Vol. 38-39, pp. 305-309 (1997)
- [12] M. Huebner, H. Meyer, K.-F. Klein, G. Hillrichs, M. Ruetting, M. Veidemanis, B. Spangenberg, J. Clarkin, G. Nelson: „Fiber-optic systems in the UV-region“. SPIE-Proc. BiOS'00, Vol. 3911, pp. 303-312 (San Jose, Jan. 2000)
- [13] K.-F.Klein,G.Hillrichs,P.Karlitschek,K.Mann: "Possibilities and limits of optical fibers for the transmission of excimer laser radiation". SPIE-Proc. Vol.2966 „Annual Boulder Damage Symposium“, pp.564-573 (Boulder, Oct. 1996)
- [14] R.S.Tayler, K.E.Leopold, R.K.Brimacombe, S.Mihailov: "Dependence of the damage and transmission properties of fused silica fibers on the excimer laser wavelength". Appl. Optics, Vol. 27 (15), pp. 3124-3134 (1988)
- [15] R.K.Brimacombe, R.S.Tayler, K.E.Leopold: "Dependence of non-linear transmission properties of fused silica fibers on the excimer laser wavelength". J.Appl. Phys., Vol. 66, pp. 4035ff (1989)

- [16] P. Karlitschek, G. Hillrichs, K.-F.Klein: „Photodegradation and nonlinear effects in optical fibers induced by pulsed UV-laser radiation“. Opt. Comm., Vol. 116, pp. 219-230 (1995)
- [17] German standardization group (DIN): proposal for first draft
- [18] G.Hillrichs, C.Gonschior, K.-F. Klein, R.Wandschneider: “Performance of low mode and single mode optical fibers for high peak power 355 nm laser radiation”. SPIE-Proc. BiOS’09, Vol. 7894, paper 7894-36 (San Jose, USA, Jan. 2009)
- [19] J.Heimann, C.P.Gonschior, K.-F.Klein, G.Hillrichs, E.Takala: “Spectral UV losses in 355 nm pulsed laser delivery system at low temperatures”. J.-Non.-Cryst.Solids, Vol. 376, pp.43-49 (2013)
- [20] CryLas GmbH, Berlin (Germany): Brochure about 266 & 355 nm Nd:YAG lasers (2014)
- [21] J&M Analytik AG, Essingen (Germany): Data sheets about Fiber-Optic Spectrometer (www.j-m.de)
- [22] Heraeus Noblelight GmbH, Hanau (Germany): Brochure about deuterium-lamps (2002)
- [23] Heraeus Quarzglas: Brochures about Suprasil™ and Fluosil™ (tradenames)
- [24] IPHT: Institute of Photonic Technology, Jena (Germany); research group “Fiber Optics”
- [25] J. Kirchhof, P.Kleinert, W. Radloff, E.Below: „Diffusion processes in lightguide materials. Status solidi (a), Vol. 101, pp. 391-401 (1987)
- [26] J.Stone: “Interactions of Hydrogen and Deuterium with Silica Optical Fibers: A Review”. IEEE J.Lightw.Techn., Vol. LT-5, pp. 712-733 (1987)
- [27] Polymicro Technologies, Phoenix (USA): Data sheets about All-Silica Fibers (www.polymicro.com)
- [28] TransMIT GmbH, Giessen (Germany): Data sheet about certified UV-fibers (2013)
- [29] K.-F. Klein, S.Pandey, P.Dahal, M.Klein, M.Belz, G.Hillrichs.: “Broadband ATR-sensor with variable pathlengths”. SPIE-Proc. BiOS’12, Vol. 8218, paper 8218-29 (San Francisco, USA, Jan. 2012)
- [30] K.-F.Klein, R.Kaminski, S.Hüttel, J.Kirchhof, S.Grimm, G.Nelson: "Lifetime improvements and of UV-improved fibers for new applicatons". SPIE-Proc.Vol. 3262C (BiOS’98), pp. 150-160 (San Jose, Jan. 1998)